Author/s:
Nathanael, JG;White, JM;Richter, A;Nuske, MR;Wille, U

Title:
Oxidative damage of proline residues by nitrate radicals (NO3): A kinetic and product study

Date:
2020-09-21

Citation:
Nathanael, J. G., White, J. M., Richter, A., Nuske, M. R. & Wille, U. (2020). Oxidative damage of proline residues by nitrate radicals (NO3): A kinetic and product study. Organic and Biomolecular Chemistry, 18 (35), pp.6949-6957. https://doi.org/10.1039/d0ob01337d.

Persistent Link:
https://hdl.handle.net/11343/299973

Organic & Biomolecular Chemistry

ROYAL SOCIETY OF CHEMISTRY

PAPER

Cite this: *Org. Biomol. Chem.*, 2020, **18**, 6949

Oxidative damage of proline residues by nitrate radicals ($NO_3^{\bullet}$): a kinetic and product study†

Joses G. Nathanael, [a] Jonathan M. White, [a] Annika Richter,[a,b] Madison R. Nuske[a] and Uta Wille *[a]

Received 30th June 2020,
Accepted 21st August 2020

DOI: 10.1039/d0ob01337d

rsc.li/obc

Tertiary amides, such as in *N*-acylated proline or *N*-methyl glycine residues, react rapidly with nitrate radicals ($NO_3^{\bullet}$) with absolute rate coefficients in the range of 4–7 × 10^8 M^{-1} s^{-1} in acetonitrile. The major pathway proceeds through oxidative electron transfer (ET) at nitrogen, whereas hydrogen abstraction is only a minor contributor under these conditions. However, steric hindrance at the amide, for example by alkyl side chains at the α-carbon, lowers the rate coefficient by up to 75%, indicating that $NO_3^{\bullet}$-induced oxidation of amide bonds proceeds through initial formation of a charge transfer complex. Furthermore, the rate of oxidative damage of proline and *N*-methyl glycine is significantly influenced by its position in a peptide. Thus, neighbouring peptide bonds, particularly in the *N*-direction, reduce the electron density at the tertiary amide, which slows down the rate of ET by up to one order of magnitude. The results from these model studies suggest that the susceptibility of proline residues in peptides to radical-induced oxidative damage should be considerably reduced, compared with the single amino acid.

Introduction

Air pollution has become the largest environmental risk for society, being responsible for the premature death of about seven million people worldwide every year.[1] In particular, the noxious gaseous pollutants nitrogen dioxide ($NO_2^{\bullet}$) and ozone (O_3) are recognised as a serious problem not only for human health[2,3] but also for plants by causing damage to cuticles and photosynthetic pigments, which reduces plant growth and productivity.[4,5] Interestingly, studies on human health effects using rat models showed that exposure to combined $NO_2^{\bullet}$ and O_3 has significant synergistic effects compared to the isolated pollutants, such as increased lipid peroxidation and protein nitration.[6] These findings suggest that highly reactive nitrate radicals ($NO_3^{\bullet}$) could be formed *in situ*, according to eqn (1):[7]

$$NO_2^{\bullet} + O_3 \rightarrow NO_3^{\bullet} + O_2 \quad (1)$$

$NO_3^{\bullet}$ is an O-centred, electrophilic and strongly oxidising radical [E° ($NO_3^{\bullet}/NO_3^{-}$) = 2.3–2.5 V *vs.* NHE],[8] which reacts with organic molecules through electron transfer (ET), addition to π systems or by hydrogen atom transfer (HAT).[7] We have recently shown through kinetic and product studies that phenylalanine, which does not react with $NO_2^{\bullet}$ or O_3 in isolation, is damaged by $NO_3^{\bullet}$ through oxidative ET at the aromatic ring.[9,10] In reactions with the less reactive aliphatic acyclic amino acids and short peptides, proton-coupled ET (PCET) at the secondary amide moiety was identified as an important reaction pathway for $NO_3^{\bullet}$, in addition to HAT from activated C–H bonds, for example from the α-carbon.[10,11]

Of the proteinogenic amino acids proline stands out due to its cyclic structure and secondary amine motif, which may lead to different reactivity towards oxidative damage, compared with the linear aliphatic amino acids (Scheme 1).

For example, recent computational studies revealed that hydroxyl radicals ($HO^{\bullet}$) could react with proline through HAT from the N–H group to form an N-centred radical **1**, which could lead to spontaneous decarboxylation of proline, or through HAT from the δ-CH_2 moiety to give radical **2**, which is

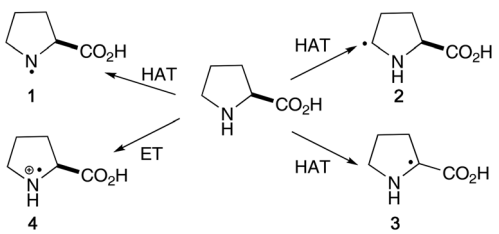

Scheme 1 Suggested radical reaction pathways in proline.

[a]*School of Chemistry, Bio21 Institute, The University of Melbourne, 30 Flemington Road, Parkville, Victoria 3010, Australia. E-mail: uwille@unimelb.edu.au*
[b]*Institute of Chemistry, Humboldt-University Berlin, Brook-Taylor-Str. 2, 12489 Berlin, Germany*

†Electronic supplementary information (ESI) available: Synthetic procedures and spectroscopic details for all substrates, details of kinetic studies, X-ray data, Gaussian archive entries. CCDC 1991811. For ESI and crystallographic data in CIF or other electronic format see DOI: 10.1039/d0ob01337d

predicted to be energetically less favourable than HAT from N–H.[12] However, when no N–H bond is present, HAT occurs from the δ-CH_2 moiety, as identified in kinetic studies of the reaction of *N*-Boc protected proline with cumyloxyl radicals ($PhCMe_2O^{\bullet}$, $CumO^{\bullet}$) in acetonitrile.[13] On the other hand, HAT from the α-position in proline to form the capto-datively stabilised α-amino acid radical **3** is only a competitive pathway in some conformations.[14] Formation of a radical cation of type **4** through oxidative ET at N has been suggested as the major pathway in reactions of amino acids with alkylated N-termini, for example *N*-methyl glycine, which can be regarded as an open-chain model for proline.[15]

Free proline is present in various organisms, where it acts as a key molecule in cell signalling, stress protection and energy production.[16] In particular, it has been found that free proline accumulates in plant tissues during abiotic stress, where it could act as a scavenger of $HO^{\bullet}$ to reduce oxidative damage caused by this radical.[17–19] However, proline's antioxidant capacity has recently been questioned because of its inability to scavenge singlet oxygen ($^1O_2$), superoxide (O_2^{-}), peroxynitrite ($ONOO^{-}$), nitric oxide ($NO^{\bullet}$) and $NO_2^{\bullet}$.[20] Irrespective of these controversies, it has been demonstrated that proline supplied at low concentrations is beneficial for the growth of plants exposed to salinity stress and decreases peroxidative damage to the lipid membranes,[17] suggesting that such application may significantly increase plant growth and crop yield under environmental stress.[21]

Proline is also an integral part of proteins, with the demand for proline in protein synthesis being the highest among all other amino acids (on a per-gram basis).[22] Given the ongoing discussion over the role of proline during salinity and drought stress, for example as essential protein building block, osmotolerant or antioxidant,[23] a fundamental understanding of radical-induced oxidative damage in proline and proline residues in peptides is essential, in particular whether and how the environment in the peptide influences the reactivity of this amino acid. In previous work, we have demonstrated that $NO_3^{\bullet}$, apart from being an important environmental oxidant, is also an excellent 'tool' to investigate irreversible radical-induced oxidative damage in biomolecules, since back-electron transfer cannot occur, which is a typical complication in studies where the oxidant is produced through photoinduced ET in donor–acceptor pairs.

Here we present the results of our kinetic and product studies of the reaction of $NO_3^{\bullet}$ with proline and proline-mimics in short peptides. Through a 'bottom-up' approach the fundamental reactivity between the biomolecule and the oxidant $NO_3^{\bullet}$ is studied without any interfering interactions with the environment (such as biological fluids or salts or even a longer peptide chain itself), which could significantly complicate data analysis and interpretation. Previous product and kinetic studies have demonstrated that acetonitrile is a highly suitable solvent for such purposes due to its low reactivity with both $NO_3^{\bullet}$ and radical intermediates formed in these reactions.[9–11] While data obtained from such model studies may not necessarily be transferable to biological conditions in their entirety,‡ having first a detailed understanding of the fundamental reactivity in model systems under exclusion of solvent interactions (the aim of this work) is crucial to minimise misinterpretation of subsequent experiments performed in more complex environments, such as in aqueous systems.§

This work reveals that the rate of proline oxidation is influenced by electron-withdrawing neighbouring amide bonds in the peptide backbone. These inductive effects should considerably reduce the susceptibility of proline residues in peptides to radical-induced oxidative damage compared with the single amino acid.

Results and discussion

Synthesis of materials and experimental set up for kinetic studies

All amino acids, di- and tripeptides studied in this work were synthesised as enantiomerically pure materials (where chiral centres are present). The purity of the compounds was confirmed by analytical HPLC. To increase the solubility in the solvent acetonitrile, all amino acids and peptides had the C-termini protected as methyl esters and the N-termini as acetamides (Ac) or phthalimides (Phth), respectively. Synthetic details and spectroscopic data for all compounds are given in the ESI.†

The nanosecond laser flash photolysis experiments were carried out at 298 ± 1 K on an Edinburgh Instrument LP920 spectrometer. The 3rd harmonic of a Quantel Brilliant B Nd:YAG laser was used to generate $NO_3^{\bullet}$ in the presence of the amino acid or short peptide through photoinduced ET from cerium(IV) ammonium nitrate (CAN) at λ = 355 nm, according to eqn (2):[7]

$$(NH_4)_2Ce(NO_3)_6 + h\nu \rightarrow NO_3^{\bullet} + (NH_4)_2Ce(NO_3)_5 \qquad (2)$$

Kinetic data for the reaction of $NO_3^{\bullet}$ with all substrates were obtained under pseudo-first order conditions by measuring the decay of the $NO_3^{\bullet}$ signal at λ = 630 nm as a function of excess amino acid, di- and tripeptide concentration, according to: $NO_3^{\bullet}$ + substrate → products, as described previously.[9e,10,11] Details of the kinetic measurements are provided in the ESI.†

Reaction of $NO_3^{\bullet}$ with tertiary amides

The obtained absolute second-order rate coefficients k for the reaction of $NO_3^{\bullet}$ with *N*-acetylated amino acids and dipeptides containing tertiary amide moieties, *i.e.*, proline

‡A linear correlation between rate coefficients for the reaction of $NO_3^{\bullet}$ with various organic compounds in water and acetonitrile has been found, with reactions in acetonitrile generally being slightly faster, see: ref. 32. While these data show that $NO_3^{\bullet}$ is highly reactive in both solvents the possibility that reaction mechanisms may be different, for example because of the different ability of these solvents to stabilise intermediates, cannot be excluded.

§This caution is justified by own previous work on the oxidation of cholesterol by $NO_2^{\bullet}$, which revealed rapid transformation of the primary products in the presence of water. Without the experiment performed in an inert solvent an incorrect radical mechanism instead of an ionic process would have been proposed, see: ref. 33.

and its open-chain model *N*-methyl glycine are in the range 10^8–10^9 M^{-1} s^{-1} (Table 1). These data are two–three orders of magnitudes higher than those for aliphatic amino acids, di- and tripeptides with secondary amide motifs,[11] suggesting that the reaction should occur through ET at the tertiary amide group. The experimental confirmation of ET as the predominant mechanism will be outlined in the next section.

The rate coefficient for the reaction of diproline (Ac-Pro-Pro-OMe, entry 2) of 16.7×10^8 M^{-1} s^{-1} is about 2.5 times higher than for proline itself (Ac-Pro-OMe, entry 1), indicating that consecutive proline residues are particularly susceptible to oxidative damage. The reactivity of proline-phenylalanine (Ac-Pro-Phe-OMe, entry 3) is with 7.2×10^8 M^{-1} s^{-1} only marginally higher than that of proline, suggesting that the reaction should take place at the proline residue only, which is supported by the much lower rate coefficient of 1.1×10^7 M^{-1} s^{-1} for the reaction of $NO_3^{\bullet}$ with phenylalanine (in Ac-Phe-OMe) determined previously.[10]

Surprisingly, the rate coefficient for the reaction of $NO_3^{\bullet}$ with the dipeptide possessing the inverted sequence, *i.e.*, Ac-Phe-Pro-OMe, is only 1.7×10^8 M^{-1} s^{-1} (entry 4). A similar outcome was obtained in glycine–proline Ac-Gly-Pro-OMe (entry 5) and leucine–proline Ac-Leu-Pro-OMe (entry 6). These findings indicate that amino acid residues in the *N*-direction could lower the electron density at the tertiary amide moiety in proline through inductive effects, thereby reducing the susceptibility of proline to radical-induced oxidative damage in peptides. This suggestion is supported by the rate coefficient for the reaction of $NO_3^{\bullet}$ with the dipeptide β-alanine–proline (Ac-βAla-Pro-OMe, entry 7), which is nearly as high as for proline itself and could be rationalised by the additional methylene group in β-alanine that dampens the electron-withdrawing effect of the N-terminal amino acid. As will be shown in the next section, HAT from the activated β-CH_2 moiety should not be competitive under these conditions. Irrespective of this, the kinetic data for Ac-βAla-Pro-OMe suggest that β-peptides, which are stable to proteolytic degradation,[24] should be significantly more prone to radical-induced oxidative damage than α-peptides, which could be one of the reasons why they are not common in nature.

The rate coefficients obtained for *N*-methyl glycine (Ac-(Me)Gly-OMe, entry 8) and *N*-methyl glycine-containing dipeptides listed in entries 9–14 show a similar trend. While the reactivity of these substrates towards $NO_3^{\bullet}$ is up to 60% lower compared with their proline counterparts, a drop of the rate coefficient by up to one order of magnitude was found when *N*-methyl glycine is the C-terminal residue in the dipeptide (entries 11–14 *vs.* 10). Overall, the data indicate that the N-terminal secondary amide pulls the electron density away from the C-terminal tertiary amide, slowing down the oxidation rate at this site.

Table 1 Absolute second-order rate coefficients *k* for the reaction of $NO_3^{\bullet}$ with *N*-acetylated amino acids and dipeptides containing proline or *N*-methyl glycine residues[a,b]

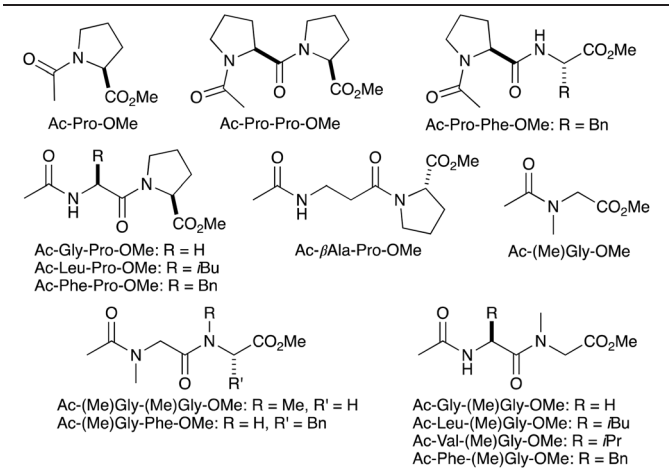

Entry	Substrate	$k/\times 10^8$ M^{-1} s^{-1}
(a) Proline and proline-containing dipeptides		
1	Ac-Pro-OMe	6.8
2	Ac-Pro-Pro-OMe	16.7
3	Ac-Pro-Phe-OMe	7.2
4	Ac-Phe-Pro-OMe	1.7
5	Ac-Gly-Pro-OMe	2.2
6	Ac-Leu-Pro-OMe	1.7
7	Ac-βAla-Pro-OMe	5.7
(b) *N*-Methyl glycine and *N*-methyl glycine-containing dipeptides		
8	Ac-(Me)Gly-OMe	4.1
9	Ac-(Me)Gly-(Me)Gly-OMe	10.6
10	Ac-(Me)Gly-Phe-OMe	6.0
11	Ac-Phe-(Me)Gly-OMe	0.8
12	Ac-Gly-(Me)Gly-OMe	0.9
13	Ac-Leu-(Me)Gly-OMe	0.6
14	Ac-Val-(Me)Gly-OMe	0.5

[a] In acetonitrile, at 298 ± 1 K. [b] Experimental error ±5%.

Mechanism: HAT *vs.* ET

Kinetic studies were performed to confirm the proposed ET mechanism as the primary pathway in the reaction of $NO_3^{\bullet}$ with tertiary amides. The results are compiled in Table 2.

We recently found that $NO_3^{\bullet}$ reacts with glycine through HAT from the α-carbon and PCET from the secondary amide moiety, with each pathway contributing 1×10^6 M^{-1} s^{-1} to the overall rate coefficient (entry 1), whereas HAT from the Me groups at both N- and C-terminus in Ac-Gly-OMe is not competitive.[10,11] The comparatively low rate coefficient for $NO_3^{\bullet}$-induced HAT from the α-carbon in α-amino acids confirms previous work by Easton, Radom and coworkers, showing that deactivating polar effects in the early, reactant-like transition state of the α-HAT disfavour this pathway for highly reactive electrophilic radicals.[25,26] However, the rate coefficient for the reaction of $NO_3^{\bullet}$ with Ac-βAla-OMe is one order of magnitude higher than for glycine (entry 2), suggesting that the reaction occurs primarily *via* HAT from the activated β-CH_2 moiety.

Because the reaction of proline with $HO^{\bullet}$ and $CumO^{\bullet}$ occurs through HAT from the δ-CH_2 group (see above),[12b,13] kinetic studies were performed to explore whether $NO_3^{\bullet}$ reacts similarly with Ac-Pro-OMe or with Ac-(Me)Gly-OMe, in the latter case through HAT from the *N*-Me group. Firstly, we investigated the $NO_3^{\bullet}$-induced HAT from an N_{amide}-CH_2 moiety using the side chain in lysine as a model system for the δ-CH_2

Table 2 Absolute second-order rate coefficients k to determine the mechanism of the reaction of $NO_3^{\bullet}$ with tertiary amide moieties in *N*-acylated amino acids[a,b]

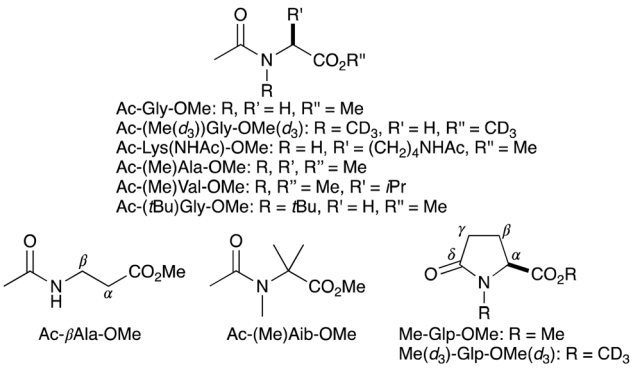

Entry	Substrate	k/× 10^8 M^{-1} s^{-1}
1	Ac-Gly-OMe	0.03[c]
2	Ac-βAla-OMe	0.3
3	Ac-Lys(NHAc)-OMe	1.0
4	Ac-(Me(d_3))Gly-OMe(d_3)	3.2
5	Me-Glp-OMe	2.0
6	Me(d_3)-Glp-OMe(d_3)	1.7
7	Ac-(Me)Ala-OMe	3.4
8	Ac-(Me)Val-OMe	2.5
9	Ac-(Me)Aib-OMe	1.4
10	Ac-(*t*Bu)Gly-OMe	1.2

[a] In acetonitrile, at 298 ± 1 K. [b] Experimental error ±10%. [c] From ref. 11.

group in Ac-Pro-OMe. Protection as a secondary amide (*i.e.*, Ac-Lys(NHAc)-OMe) was performed to both lower its susceptibility to ET by $NO_3^{\bullet}$ and to mimic *N*-acetylation in Ac-Pro-OMe. The rate coefficient of 1×10^8 M^{-1} s^{-1} obtained for the reaction of $NO_3^{\bullet}$ with this amino acid (entry 3) clearly suggests a fast HAT process at the N_{amide}-CH_2 motif remote to the electron-withdrawing carboxyl group. Assuming that the HAT reaction from both secondary and tertiary N_{amide}-CH_2 moieties are approximately similar, the nearly seven times higher reactivity of Ac-Pro-OMe (Table 1, entry 1) suggests that HAT is only a minor contributor to the overall reaction. Therefore, the major pathway should proceed *via* $NO_3^{\bullet}$-induced ET at the tertiary amide moiety, for which an upper limit of *ca.* 5.8×10^8 M^{-1} s^{-1} can be tentatively given.

Next, HAT from the tertiary N_{amide}-CH_3 group in Ac-(Me)Gly-OMe was examined through deuterium kinetic isotope studies for the pairs Ac-(Me)Gly-OMe/Ac-(Me(d_3))Gly-OMe(d_3) (Table 1, entry 8 *vs.* Table 2, entry 4), and of *N*-methylpyroglutamic methylester, *i.e.*, Me-Glp-OMe/Me(d_3)-Glp-OMe(d_3) (Table 2, entry 5 *vs.* 6). A value of $k_H/k_D = 1.2$ was obtained for both substrate pairs, which indicates that HAT contributes only to a minor extent to the overall reaction.¶

¶It should be noted that low k_H/k_D values could also indicate a highly non-symmetrical (very early or very late) transition state. However, previous computational studies of reactions of $NO_3^{\bullet}$ with aliphatic amino acids (see ref. 11) suggest that such unsymmetrical transition states are not likely in the reactions studied in this work.

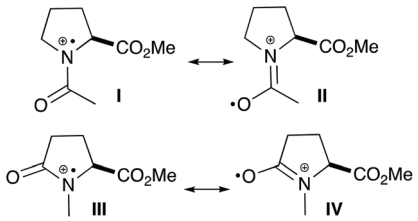

Scheme 2 Resonance structures of the amide radical cations of Ac-Pro-OMe (I and II) and Me-Glp-OMe (III and IV).

From the rate differences between the deuterated and non-deuterated substrates, the rate coefficient for the $NO_3^{\bullet}$-induced HAT from N_{amide}-CH_3 can be estimated as $(6 \pm 3) \times 10^7$ M^{-1} s^{-1}, leading to a rate coefficient of about 3.5×10^8 M^{-1} s^{-1} for the ET reaction at the tertiary amide moiety in Ac-(Me)Gly-OMe.

The three times higher reactivity of Ac-Pro-OMe compared with Me-Glp-OMe (Table 1, entry 1 *vs.* Table 2, entry 5) is noteworthy, since both are cyclic amino acids with similar functional groups. A possible rationale is provided in Scheme 2, which shows that the radical cation **I** formed through ET in Ac-Pro-OMe is stabilised through resonance involving the exocyclic acetyl group (**II**). On the other hand, resonance stabilisation of the radical cation of Me-Glp-OMe (**III**) *via* **IV** requires planarisation of the amide moiety within the 5-membered ring, which increases ring strain and should therefore decrease the rate of oxidation.

Interestingly, the data in Table 2 also show that the rate coefficients for the $NO_3^{\bullet}$-induced ET of *N*-methylated amino acids decreased with increasing steric demand at the α-carbon, dropping from 4.1×10^8 for the unhindered Ac-(Me)Gly-OMe (Table 1, entry 8), to 3.4×10^8 for alanine (Ac-(Me)Ala-OMe, entry 7), 2.5×10^8 for valine (Ac-(Me)Val-OMe, entry 8) and to 1.4×10^8 M^{-1} s^{-1} for the most sterically hindered 2-aminoisobutyric acid (Ac-(Me)Aib-OMe, entry 9). A similar outcome was obtained for Ac-(*t*Bu)Gly-OMe (entry 10), where the bulky *t*-butyl substituent at the amide led to a drop of the rate coefficient to only 25% of that of Ac-(Me)Gly-OMe. Because the *t*-butyl group is inert towards $NO_3^{\bullet}$-induced HAT,[11] it would be expected that its larger inductive effect, compared with that of a methyl group, should facilitate amide oxidation. The opposite outcome clearly shows that the rate of $NO_3^{\bullet}$-induced oxidation of tertiary amides is influenced by their accessibility for approach by $NO_3^{\bullet}$, confirming earlier findings for the PCET reaction with secondary amides, which proceeds through initial formation of a CT complex.[11]

ET at tertiary amides in peptides – the role of inductive effects

To further explore the role of the N-terminal amino acid on the ET rate at a tertiary amide, kinetic studies were performed for the reaction of $NO_3^{\bullet}$ with a series of model di- and tripeptides containing a C-terminal *N*-methyl glycine. The N-terminus was protected as an electron-withdrawing phthalimide to exclude ET at this site, to reduce the susceptibility of the adjacent α-C–H bonds to HAT,[27] and to provide a strong electron-pull on the

Table 3 Absolute second-order rate coefficients k for the reaction of $NO_3^{\bullet}$ with *N*-phthaloylated di- and tripeptides possessing *N*-methyl glycine residues[a,b]

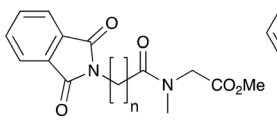

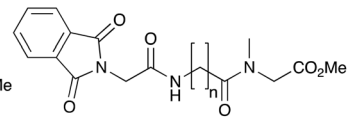

n = 1:	Phth-Gly-(Me)Gly-OMe	Phth-Gly-Gly-(Me)Gly-OMe
n = 2:	Phth-βAla-(Me)Gly-OMe	Phth-Gly-βAla-(Me)Gly-OMe
n = 3:	Phth-Gaba-(Me)Gly-OMe	Phth-Gly-Gaba-(Me)Gly-OMe
n = 4:	Phth-Ava-(Me)Gly-OMe	Phth-Gly-Ava-(Me)Gly-OMe
n = 5:	Phth-Ahx-(Me)Gly-OMe	Phth-Gly-Ahx-(Me)Gly-OMe

Entry	Substrate	$k/\times 10^8$ M^{-1} s^{-1}
1[c]	Phth-Gly-(Me)Gly-OMe	0.2
2	Phth-βAla-(Me)Gly-OMe	2.0
3	Phth-Gaba-(Me)Gly-OMe	3.7
4	Phth-Ava-(Me)Gly-OMe	4.8
5	Phth-Ahx-(Me)Gly-OMe	5.6
6	Phth-Gly-Gly-(Me)Gly-OMe	0.6
7	Phth-Gly-βAla-(Me)Gly-OMe	2.2
8	Phth-Gly-Gaba-(Me)Gly-OMe	3.6
9	Phth-Gly-Ava-(Me)Gly-OMe	4.6
10[c]	Phth-Gly-Ahx-(Me)Gly-OMe	5.6

[a] In acetonitrile, at 298 ± 1 K. [b] Experimental error ±5%, unless stated otherwise. [c] Experimental error ±10%.

adjacent bonds. In the dipeptide series, *N*-methyl glycine was separated from the *N*-phthalimide terminus through amino acids with 1–5 methylene units, *i.e.*, Gly (n = 1), β-Ala (n = 2), γ-aminobutyric acid (Gaba, n = 3), δ-aminovaleric acid (Ava, n = 4) and ε-aminocaproic acid (Ahx, n = 5). Likewise, in the tripeptide series the N-terminal phthaloyl glycine and the C-terminal *N*-methyl glycine were separated by Gly, β-Ala, Gaba, Ava and Ahx, respectively. The obtained rate coefficients are given in Table 3.

Comparison of the data for the reaction of $NO_3^{\bullet}$ with Phth-Gly-(Me)Gly-OMe (entry 1) with those for Ac-(Me)Gly-OMe (Table 1, entry 8) shows a drop in reactivity by a factor of 20, clearly revealing the deactivating effect of the N-terminal phthaloyl glycine on the tertiary amide in *N*-methyl glycine.‖ Increasing the distance between the tertiary amide and phthalimide moieties by just one additional CH_2 group leads to a significant increase of the rate coefficient by one order of magnitude to 2.0×10^8 M^{-1} s^{-1} (entry 2). Further separation of these two groups further increases the reactivity but to a much lesser extent, reaching 5.6×10^8 M^{-1} s^{-1} for the longest linker in Phth-Ahx-(Me)Gly-OMe (entry 5).

A similar behaviour was found for the tripeptide series shown in entries 6–10, where the biggest 'jump' in reactivity by a factor of about four occurred in going from Gly to β-Ala as the separating amino acid. It should be noted that the three

‖ The rate coefficients for the reactions of $NO_3^{\bullet}$ with the *N*-phthaloylated amino acids Gly, βAla, Gaba, Ava and Ahx, which likely proceed through HAT from the various CH_2 moieties, are lower and in the range $0.6–1.6 \times 10^6$ M^{-1} s^{-1} (data are given in the ESI, Table S1†).

Table 4 Absolute second-order rate coefficients k for the reaction of $NO_3^{\bullet}$ with *N*-phthaloylated dipeptides possessing secondary amide moieties[a,b]

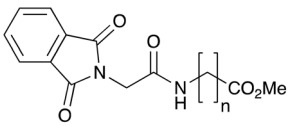

n = 1:	Phth-Gly-Gly-OMe
n = 2:	Phth-Gly-βAla-OMe
n = 3:	Phth-Gly-Gaba-OMe
n = 4:	Phth-Gly-Ava-OMe
n = 5:	Phth-Gly-Ahx-OMe

Entry	Substrate	$k/\times 10^6$ M^{-1} s^{-1}
1	Phth-Gly-Gly-OMe	1.5
2	Phth-Gly-βAla-OMe	3.7
3	Phth-Gly-Gaba-OMe	7.8
4	Phth-Gly-Ava-OMe	10.3
5	Phth-Gly-Ahx-OMe	13.1

[a] In acetonitrile, at 298 ± 1 K. [b] Experimental error ±10%.

times higher reactivity of Phth-Gly-Gly-(Me)Gly-OMe towards $NO_3^{\bullet}$ (entry 6) compared with Phth-Gly-(Me)Gly-OMe (entry 1) is due to the extra glycine residue that separates the electron-withdrawing phthaloyl group from the tertiary amide in the former. Interestingly, this difference in reactivity is already eradicated by only one additional CH_2 group in the carbon linker (entries 2 *vs.* 7).

To explore the role of the *C*-direction amino acid on the rate of amide oxidation by $NO_3^{\bullet}$, we used dipeptides with a central secondary amide moiety as the site for PCET and an N-terminal glycine, which was deactivated for radical attack through *N*-phthalimide protection. The data in Table 4 reveal a gradual increase of the rate coefficient with increasing distance between the C-terminal ester and the amide motif.

However, compared with an electron-withdrawing N-terminus, where the rate coefficient increased by one order of magnitude in going from Gly to β-Ala as the spacer amino acid (see Table 3), the rate coefficient increased with increments of only *ca.* $(3 \pm 1) \times 10^6$ M^{-1} s^{-1} for each additional CH_2 moiety that separates the amide from the electron-withdrawing C-terminus.

Although it is not possible to exclude that HAT from the N_{amide}-CH_2 group might also occur to some extent, this data nevertheless shows that reactions at the amide moiety itself are slowed down by negative inductive effects caused by the C-terminus, however to a much lesser extent than those caused by electron-withdrawing groups in the *N*-direction.

Product studies

We were interested to explore whether the position-dependent oxidation rate of proline is also reflected by different reaction outcomes and analysed the products formed in the reaction of $NO_3^{\bullet}$ with the isomeric dipeptides Ac-Pro-Phe-OMe and Ac-Phe-Pro-OMe. For these experiments $NO_3^{\bullet}$ was generated

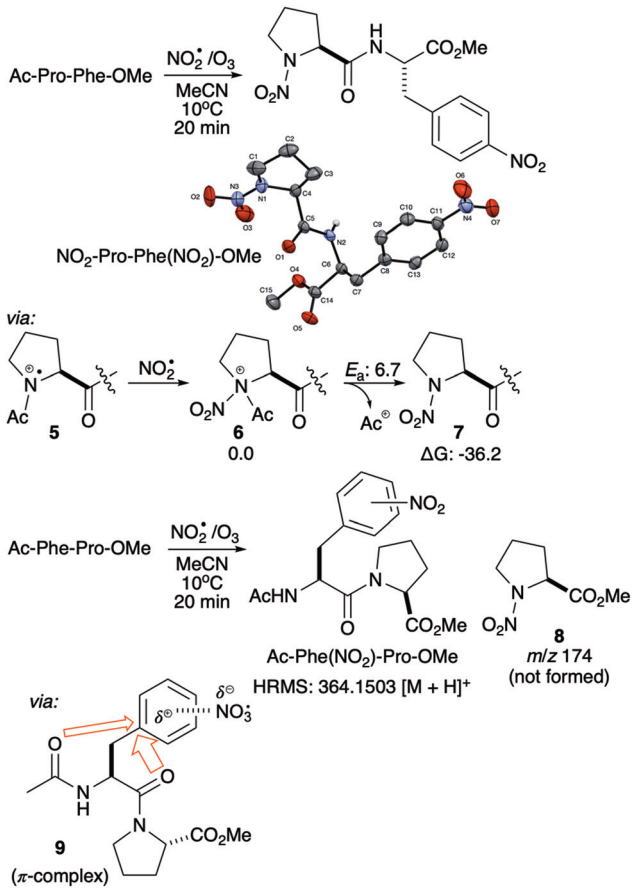

Scheme 3 Reaction of Ac-Pro-Phe-OMe and Ac-Phe-Pro-OMe with $NO_3^{\bullet}$ generated by reaction of $NO_2^{\bullet}$ with O_3. Free energies in kJ mol^{-1}, calculated with M062X/6-31+G* in acetonitrile.

in situ in acetonitrile through the reaction of $NO_2^{\bullet}$ with O_3 (see eqn (1)) in the presence of the substrate, using experimental conditions developed previously by us.** [9c,d] Details are given in the ESI.†

The reaction of Ac-Pro-Phe-OMe led to formation of the dinitro derivative NO_2-Pro-Phe(NO_2)-OMe in which the *N*-acetyl group was replaced by NO_2 and the Phe residue converted into 4-nitro phenylalanine, as confirmed by the X-ray structure (Scheme 3). When a lower amount of $NO_2^{\bullet}$ was used, only mononitration of Ac-Pro-Phe-OMe was observed. Analysis by ESI-HRMS indicated that the major product was the *N*-nitro proline dipeptide NO_2-Pro-Phe-OMe (calcd for $[C_{15}H_{19}N_3O_5]^+$: 322.1398 $[M + H]^+$, found 322.1395) in which the Phe residue remained unchanged (not shown). The result is consistent with the kinetic studies where the Pro residue is found to be more reactive than Phe in acetonitrile. Control experiments showed that no reaction occurred with Ac-Pro-Phe-OMe in the absence of O_3 (see ESI†).

As mentioned in the Introduction, reaction at the aromatic ring in Phe is initiated through ET by $NO_3^{\bullet}$, which under these conditions is followed by recombination of the arene radical cation with residual $NO_2^{\bullet}$ and deprotonation.†† [9,10] A similar process likely occurs also at the Pro residue in Ac-Pro-Phe-OMe, where oxidation of the tertiary amide by $NO_3^{\bullet}$ leads to the radical cation **5**, which is trapped by $NO_2^{\bullet}$ to form the cationic intermediate **6**. Subsequent heterolytic cleavage of the *N*-acetyl bond leads to the *N*-nitro proline residue **7**. This suggestion was supported by density functional theory (DFT) studies (see Experimental section), which showed a modest barrier for the loss of Ac^+ in **6** of about 7 kJ mol^{-1} and a considerable exothermicity of this step by *ca.* 36 kJ mol^{-1}. For comparison, heterolytic loss of NO_2^+ in **6**, which would restore the undamaged Ac-Pro moiety, is associated with a barrier of 62.6 kJ mol^{-1} and is endothermic by 9.9 kJ mol^{-1} (not shown).

On the other hand, the reaction of Ac-Phe-Pro-OMe with $NO_3^{\bullet}$ led to several products, of which the major product could be tentatively assigned by ESI-HRMS as the nitro derivative Ac-Phe(NO_2)-Pro-OMe (calcd for $[C_{17}H_{22}N_3O_6]^+$: 364.1504 $[M + H]^+$, found 364.1503). Reaction through oxidation of the Pro residue would be expected to lead to formation of the *N*-nitro proline derivative **8** through cleavage of the peptide bond (similar to the reaction with Ac-Pro-Phe-OMe). However, no product of this mass (either deprotonated or protonated) was found in the mass spectrum of the reaction mixture (see ESI†), indicating that oxidation of the Pro residue did not occur to a measurable extent.

The selectivity for a reaction at the N-terminal Phe in Ac-Phe-Pro-OMe is in line with our previous findings that oxidation of the aromatic ring in Phe is significantly facilitated by neighbouring amide groups, which stabilise the developing positive charge on the aromatic ring through formation of a π-complex.[9e] Phe oxidation in Ac-Phe-Pro-OMe should even be easier, since the nucleophilic tertiary amide of the C-terminal Pro residue should provide more stabilisation in the π-complex **9** (Scheme 3) than a secondary amide.

Overall, the data suggest that the reduced susceptibility of the Pro residue in Ac-Phe-Pro-OMe for $NO_3^{\bullet}$-induced oxidation is due to two effects that remove the electron density from the tertiary amide: (i) the electron-withdrawing N-terminal amide moiety, and (ii) participation in a π-complex that facilitates Phe oxidation. On the other hand, in peptide sequences where Pro is flanked by aliphatic amino acids and such π-complexes are not formed, deactivation of the tertiary amide by neighbouring N-terminal amide bonds is the dominant factor that lowers the susceptibility of Pro residues to oxidation.

**Reaction of these dipeptides with $NO_3^{\bullet}$ generated from CAN by irradiation with 350 nm light in a Rayonet photoreactor gave a large number of products, which presumably resulted from subsequent photochemical decomposition and were not identified.

††The $NO_2^{\bullet}/O_3$-mediated nitration of Phe leads to nitroaromatic products with *o*/*m*/*p* ratios similar to the electrophilic aromatic nitration (see ref. 9 and 10). Regioisomeric products were also formed in the reaction of Ac-Pro-Phe-OMe, but only the major 4-nitro product could be separated by column chromatography, followed by recrystallisation.

Conclusions

This model study revealed that $NO_3^{\bullet}$ reacts in acetonitrile with tertiary amides, such as proline residues in peptides, predominantly by oxidative ET at the nitrogen, whereas HAT from the δ-CH_2 group is only a minor pathway. This mechanism highlights the strong oxidising capacity of $NO_3^{\bullet}$ and contrasts that of other O-centred radicals, such as $HO^{\bullet}$, which react with proline through HAT. The rate of $NO_3^{\bullet}$-induced ET is considerably influenced by steric hindrance at the tertiary amide, where bulky substituents, for example a *t*-butyl group on the amide nitrogen or alkyl side chains at the α-carbon in a peptide, diminish the oxidation rate by up to 75%. These results support earlier findings that $NO_3^{\bullet}$-induced oxidation of amide bonds in peptides proceeds through initial formation of a CT complex,[11] which becomes more difficult when steric bulk at the amide hinders approach by $NO_3^{\bullet}$.

N-Acylated proline is more than two orders of magnitude more reactive towards $NO_3^{\bullet}$ than linear *N*-acylated aliphatic amino acids, highlighting the role of the tertiary amide moiety that results from its cyclic structure. While removal of the N-protecting group would be expected to increase the electron density at nitrogen, thereby rendering free or N-terminal proline in peptides even more susceptible to oxidation by $NO_3^{\bullet}$, further experiments are clearly required to test this hypothesis (see below). On the other hand, nearby electron-withdrawing groups, such as neighbouring amide bonds in peptides, reduce the electron density of the tertiary amide in proline and *N*-methyl glycine residues and slow down the rate of ET. Although this rate retardation is caused by amide bonds in both *N*- and *C*-direction, the deactivating effect of N-terminal peptide bonds is considerably stronger. The kinetic data are supported by products studies, which showed that $NO_3^{\bullet}$-induced oxidation of proline occurs in Ac-Pro-Phe-OMe but not in the dipeptide with the inverted sequence Ac-Phe-Pro-OMe. The diminished reactivity of the tertiary amide of Pro in the latter dipeptide is due to the deactivating effect caused by the N-terminal amide moiety, in addition to formation of a π-complex that facilitates oxidation of the Phe residue through neighbouring amide group effects.[9e]

While the data in this work clearly suggest that nearby amide bonds could protect proline residues in peptides against radical-induced oxidative damage (at least to some extent), we wish to re-iterate the model character of this study. Interactions with the environment, including hydrogen bonding between the peptide and solvent, were minimised on purpose to enable insight into the fundamental reactivity of proline towards radical oxidation. These data provide the required foundation for the next phase of our studies, where the role of an aqueous environment, in particular hydrogen bonding, on radical-induced oxidative damage of proline as both single amino acid (without and with N-protection) and in short peptides will be explored. This work is currently ongoing in our laboratory, and we will report on the findings in due course.

Experimental

Synthesis of the starting materials

All compounds used in the kinetic and products studies were prepared according to established procedures. Synthetic details and spectroscopic data are given in the ESI.†

Kinetic studies

The kinetic experiments were performed at 298 ± 1 K on an Edinburgh Instrument LP920 spectrometer described previously,[9e,10,11] using the third harmonic of a Quantel Brilliant B Nd:YAG laser (6 ns pulse, 10–20 mJ, λ = 355 nm) to generate the reaction transient. The detection system employed a Hamamatsu R2856 photomultiplier tube (PMT) interfaced with a Tektronix TDS 3012C Digital Phosphor oscilloscope for transient absorption spectra. Kinetic measurements were carried out under pseudo-first order conditions following the established procedure described in ref. 10. Measurements for each substrate were done in triplicate and the results are reported as the average of these three runs. Experimental details of the kinetic measurements and data evaluation are given in the ESI (Fig. S1–S8†).

Computational studies

The computations were carried out with the Gaussian 09 program[28] using the M062X method[29] in combination with the 6-31+G* basis set, which has been employed previously to investigate radical induced damage in amino acids.[10,11] Calculations in acetonitrile were performed using the Conductor-like Polarizable Continuum Model (CPCM) for acetonitrile.[30] The ground and transition structures were verified by vibrational frequency analysis at the same level of theory, and all identified transition structures showed only one imaginary frequency. The Gaussian archive entries, including free energy data and imaginary frequency of the transition structure, are given in the ESI.†

Crystal data for NO_2-Pro-Phe(NO_2)-OMe

$C_{15}H_{18}N_4O_7$ M = 366.33, T = 130.0(2) K, λ = 1.54184 Å, monoclinic, space group $P2_1$, a = 4.7625(2), b = 13.0451(8), c = 13.8262(10) Å, β = 95.126(5)°, V = 855.55(9) Å^3, Z = 2, D_c = 1.422 Mg M^{-3}, m(Cu-Kα) = 0.977 mm^{-1}, F(000) = 384, crystal size 0.5 × 0.06 × 0.02 mm. θ_{max} = 74.73°, 4959 reflections measured, 2723 independent reflections (R_{int} = 0.0400) the final R = 0.0447[$I > 2\sigma(I)$, 2335 data] and wR($F2$) = 0.1183 (all data) GOOF = 1.070. CCDC deposit code 1991811.† Further details are provided in the ESI.†

Conflicts of interest

There are no conflicts to declare.

Acknowledgements

This work was supported by the Australian Research Council through the Linkage, Infrastructure, Equipment and Facilities

(LIEF) Grant Scheme and The University of Melbourne through the High-Performance Computing facility.[31]

Notes and references

1 J. Lelieveld, J. S. Evans, M. Fnais, D. Giannadaki and A. Pozzer, *Nature*, 2015, **525**, 367.

2 L. Trasande and G. D. Thurston, *J. Allergy Clin. Immunol.*, 2005, **115**, 690.

3 R. Ehrlich, *Environ. Health Perspect.*, 1980, **35**, 89; H. Bayram, R. J. Sapsford, M. M. Abdellaziz and O. A. Khair, *J. Allergy Clin. Immunol.*, 2001, **107**, 287; J. Sunyer, X. Basagña, J. Belmonte and J. M. Antó, *Thorax*, 2002, **57**, 687; A. J. Chauhan and S. L. Johnston, *Br. Med. Bull.*, 2003, **68**, 95.

4 W. E. Winner and C. J. Atkinson, *Trends Ecol. Evol.*, 1986, **1**, 15.

5 S. Tiwari, M. Agrawal and F. M. Marshall, *Environ. Monit. Assess.*, 2006, **119**, 15; P. C. Joshi and A. Swami, *J. Environ. Biol.*, 2009, **30**, 295.

6 Selected examples: R. Ehrlich, J. C. Findlay and D. E. Gardner, *J. Toxicol. Environ. Health*, 1979, **5**, 631; T. Ichinose and M. Sagai, *Toxicology*, 1989, **59**, 259; T. Franze, M. G. Weller, R. Niessner and U. Pöschl, *Environ. Sci. Technol.*, 2005, **39**, 1673.

7 R. P. Wayne, I. Barnes, P. Biggs, J. P. Burrows, C. E. Canosa-Mas, J. Hjorth, G. Le Bras, G. K. Moortgat, D. Perner, G. Restelli and H. Sidebottom, *Atmos. Environ., Part A*, 1991, **25**, 1.

8 P. Neta, R. E. Huie and A. B. Ross, *J. Phys. Chem. Ref. Data*, 1988, **17**, 1027.

9 (*a*) D. C. E. Sigmund and U. Wille, *Chem. Commun.*, 2008, 2121; (*b*) C. Goeschen, N. Wibowo, J. W. White and U. Wille, *Org. Biomol. Chem.*, 2011, **9**, 3380; (*c*) L. F. Gamon, J. M. White and U. Wille, *Org. Biomol. Chem.*, 2014, **12**, 8280; (*d*) L. F. Gamon and U. Wille, *Acc. Chem. Res.*, 2016, **49**, 2134; (*e*) J. G. Nathanael, L. F. Gamon, M. Cordes, P. R. Rablen, T. Bally, K. F. Fromm, B. Giese and U. Wille, *ChemBioChem*, 2018, **19**, 922.

10 J. G. Nathanael, A. N. Hancock and U. Wille, *Chem. – Asian J.*, 2016, **11**, 3188.

11 J. G. Nathanael and U. Wille, *J. Org. Chem.*, 2019, **84**, 3405.

12 (*a*) S. Signorelli, P. D. Dans, E. L. Coitiño, O. Borsani and J. Monza, *PLoS One*, 2015, **10**, e0115349; (*b*) S. Signorelli, E. L. Coitiño, O. Borsani and J. Monza, *J. Phys. Chem. B*, 2014, **118**, 37.

13 B. Salamone, F. Basili and M. Bietti, *J. Org. Chem.*, 2015, **80**, 3643.

14 B. Chan and L. Radom, *Aust. J. Chem.*, 2018, **71**, 257.

15 I. Štefanić, M. Bonifačić, K. Asmus and D. A. Armstrong, *J. Phys. Chem. A*, 2001, **105**, 8681.

16 A. A. Morgan and E. Rubenstein, *PLoS One*, 2013, **8**, 1; S. L. Christgen and D. F. Becker, *Antioxid. Redox Signal.*, 2018, **30**, 1.

17 D. Roy, N. Basu, A. Bhunia and S. K. Banerjee, *Biol. Plant.*, 1993, **35**, 69; S. Hayat, Q. Hayat, M. N. Alyemeni, A. S. Wani, J. Pichtel and A. Ahmad, *Plant Signaling Behav.*, 2012, **7**, 1456.

18 S. Kaul, S. S. Sharma and I. K. Mehta, *Amino Acids*, 2008, **34**, 315.

19 N. Smirnoff and Q. J. Cumbes, *Phytochemistry*, 1989, **28**, 1057.

20 S. Signorelli, J. B. Arellano, T. B. Melø, O. Borsani and J. Monza, *Plant Physiol. Biochem.*, 2013, **64**, 80; S. Signorelli, C. Imparatta, M. Rodríguez-Ruiz, O. Borsani, F. J. Corpas and J. Monza, *Funct. Plant Biol.*, 2016, **43**, 870.

21 M. Ashraf and M. R. Foolad, *Environ. Exp. Bot.*, 2007, **59**, 206.

22 G. Wu, F. W. Bazer, R. C. Burghardt, G. A. Johnson, S. W. Kim, D. A. Knabe, P. Li, X. Li, J. R. McKnight, M. C. Satterfield and T. E. Spencer, *Amino Acids*, 2011, **40**, 1053.

23 S. C. Chun, M. Paramasivan and M. Chandrasekaran, *Front. Microbiol.*, 2018, **9**, 2525.

24 T. Beke, C. Somlai and A. Perscel, *J. Comput. Chem.*, 2006, **27**, 20.

25 (*a*) Z. I. Watts and C. J. Easton, *J. Am. Chem. Soc.*, 2009, **131**, 11323; (*b*) B. N. Nukuna, M. B. Goshe and V. E. Anderson, *J. Am. Chem. Soc.*, 2001, **123**, 1208; (*c*) M. B. Goshe, Y. H. Chen and V. E. Anderson, *Biochemistry*, 2000, **39**, 1761.

26 (*a*) B. Chan, R. J. O'Reilly, C. J. Easton and L. Radom, *J. Org. Chem.*, 2012, **77**, 9807; (*b*) R. J. O'Reilly, B. Chan, M. S. Taylor, S. Ivanic, G. B. Bacskay, C. J. Easton and L. Radom, *J. Am. Chem. Soc.*, 2011, **133**, 16553.

27 J. Ho, M. L. Coote and C. J. Easton, *Aust. J. Chem.*, 2011, **64**, 403; A. K. Croft, C. J. Easton and L. Radom, *J. Am. Chem. Soc.*, 2003, **125**, 4119; C. J. Easton, C. A. Hutton, G. Rositano and E. W. Tan, *J. Org. Chem.*, 1991, **56**, 5614; A. K. Croft, C. J. Easton, K. Kociuba and L. Radom, *Tetrahedron: Asymmetry*, 2003, **14**, 2919.

28 M. J. Frisch, G. W. Trucks, H. B. Schlegel, G. E. Scuseria, M. A. Robb, J. R. Cheeseman, G. Scalmani, V. Barone, B. Mennucci, G. A. Petersson, H. Nakatsuji, M. Caricato, X. Li, H. P. Hratchian, A. F. Izmaylov, J. Bloino, G. Zheng, J. L. Sonnenberg, M. Hada, M. Ehara, K. Toyota, R. Fukuda, J. Hasegawa, M. Ishida, T. Nakajima, Y. Honda, O. Kitao, H. Nakai, T. Vreven, J. A. Montgomery Jr., J. E. Peralta, F. Ogliaro, M. Bearpark, J. J. Heyd, E. Brothers, K. N. Kudin, V. N. Staroverov, T. Keith, R. Kobayashi, J. Normand, K. Raghavachari, A. Rendell, J. C. Burant, S. S. Iyengar, J. Tomasi, M. Cossi, N. Rega, J. M. Millam, M. Klene, J. E. Knox, J. B. Cross, V. Bakken, C. Adamo, J. Jaramillo, R. Gomperts, R. E. Stratmann, O. Yazyev, A. J. Austin, R. Cammi, C. Pomelli, J. W. Ochterski, R. L. Martin, K. Morokuma, V. G. Zakrzewski, G. A. Voth, P. Salvador, J. J. Dannenberg, S. Dapprich, A. D. Daniels, O. Farkas, J. B. Foresman, J. V. Ortiz, J. Cioslowski and D. J. Fox, *Gaussian 09, Revision B.01*, Gaussian, Inc., Wallingford CT, 2010.

29 Y. Zhao and D. G. Truhlar, *Theor. Chem. Acc.*, 2008, **120**, 215; L. Goerigk, A. Hansen, C. Bauer, S. Ehrlich, A. Najibi and S. Grimme, *Phys. Chem. Chem. Phys.*, 2017, **19**, 32184; L. Goerigk and S. Grimme, *Phys. Chem. Chem. Phys.*, 2011, **13**, 6670.
30 Y. Takano and K. N. Houk, *J. Chem. Theory Comput.*, 2005, **1**, 70.
31 B. Meade, L. Lafayette, G. Sauter and D. Tosello, *Spartan HPC-Cloud Hybrid: Delivering Performance and Flexibility*, University of Melbourne, 2017, DOI: 10.4225/49/58ead90dceaaa.
32 S. P. Mezyk, T. D. Cullen, K. A. Rickman and B. J. Mincher, *Int. J. Chem. Kinet.*, 2017, **49**, 635.
33 A. Zalewski, J. G. Nathanael, J. M. White and U. Wille, *Chem. Commun.*, 2016, **52**, 4060.